Estimating regional greenhouse gas fluxes: An uncertainty analysis of planetary boundary layer techniques and bottom-up inventories

Xin Zhang[1*], Xuhui Lee[1,2], Timothy J. Griffis[3], John M. Baker[4], Wei Xiao[2]

1: School of Forestry and Environmental Studies, Yale University, New Haven, CT, USA.

2: Yale-NUIST Center on Atmospheric Environment, Nanjing University of Information Science and Technology, Nanjing, Jiangsu, China.

3: Department of Soil, Water, and Climate, University of Minnesota, Saint Paul, MN, USA.

4: Agricultural Research Service, USDA, Saint Paul, MN, USA.

Corresponding author: Xin Zhang, Woodrow Wilson School of Public and International Affairs, Princeton University, Princeton, NJ, USA, tel. +1 203 859 1211, email: xz2@princeton.edu

*: Now at Woodrow Wilson School of Public and International Affairs, Princeton University, Princeton, NJ, USA

Abstract

Quantification of regional greenhouse gas (GHG) fluxes is essential for establishing mitigation strategies and evaluating their effectiveness. Here, we used multiple top-down approaches and multiple trace gas observations at a tall tower to estimate regional-scale GHG fluxes and evaluate the GHG fluxes derived from bottom-up approaches. We first applied the eddy covariance, equilibrium, inverse modeling (CarbonTracker), and flux aggregation methods using three years of carbon dioxide (CO_2) measurements on a 244-meter tall tower in the Upper Midwest, USA. We then applied the equilibrium method for estimating CH_4 and N_2O fluxes with one-month high-frequency CH_4 and N_2O gradient measurements on the tall tower and one-year concentration measurements on a nearby tall tower, and evaluated the uncertainties of this application. The results indicate that: 1) The flux aggregation, eddy covariance, the equilibrium method, and the CarbonTracker product all gave similar seasonal patterns of the regional CO_2 flux (10^5-10^6 km^2), but that the equilibrium method underestimated the July CO_2 flux by 52-69%. 2) The annual budget varied among these methods from -54 to -131 g C-CO_2 m^{-2} yr^{-1}, indicating a large uncertainty in the annual CO_2 flux estimation. 3) The regional CH_4 and N_2O emissions according to a top-down method were at least six and two times higher than the emissions from a bottom-up inventory (Emission Database for Global Atmospheric Research), respectively. 4) The global warming potentials of the CH_4 and N_2O emissions were equal in magnitude to the cooling benefit of the regional CO_2 uptake. The regional GHG budget, including both biological and anthropogenic origins, is estimated at 7 ± 160 g CO_2 eq m^{-2} yr^{-1}.

Keywords: eddy covariance; equilibrium method; greenhouse gas; inverse method; land surface flux; tall tower

1. Introduction

Although quantifying GHG fluxes at the regional scale (10^2-10^6 km^2) is essential for coordinating GHG mitigation strategies, observations and flux information at these relevant scales are still extremely limited (e.g., Chen et al., 2008; Nisbet and Weiss, 2010). To fill this scale gap, some researchers build ecosystem models and aggregate the modeled flux according to land information (e.g., Desai et al., 2008; Tang et al., 2012; Xiao et al., 2008), while others use GHG concentration observations in combination with atmospheric transport models to derive the land surface flux (Lauvaux et al., 2012; Peters et al., 2007). The aggregation method is a bottom-up approach. Another bottom-up method is the IPCC national GHG inventory system (IPCC, 2006) based on emission factors and data concerning anthropogenic activities. The bottom-up applications are relatively easy to implement; however, they require independent verification, because uncertainties in land cover, anthropogenic activity, vegetation flux, and emission factors can lead to large biases (Chen et al., 2008; Levy et al., 1999). Hence, there is a strong motivation for using top-down methods to provide an independent constraint on the regional fluxes.

There are several top-down methods for estimating regional GHG fluxes, including tall-tower eddy covariance (Davis et al., 2003), the equilibrium boundary layer approach (Bakwin et al., 2004; Betts et al., 2004; Desai et al., 2010; Helliker et al., 2004), and inverse modeling (Peters et al., 2007). Each method uses different assumptions, has inherent advantages and disadvantages, and is sensitive to different parameters. Eddy covariance (EC) provides a direct measurement of the flux using measurement of the wind fluctuations and the scalar of interest. EC has been used for CO_2 flux measurement on tall towers (Davis et al., 2003; Haszpra et al., 2005), while few tall-tower flux observations of CH_4 and N_2O have been carried out due to instrument limitations (Desai et al., 2012) and the relatively large uncertainty for these measurements (20–300% for

60 CH_4, 30–1800% for N_2O) (Kroon et al., 2010). Based on the mass balance in the atmospheric
61 boundary layer, the equilibrium method assumes that the exchange at the top of the boundary
62 layer and the exchange at the land surface are in equilibrium over periods longer than about 1
63 month (Betts, 2000). The largest source of uncertainty of this method lies in determining the
64 background concentration above the boundary layer and the entrainment rate at the top of the
65 boundary layer. Inverse modeling determines the land surface flux using atmospheric transport
66 models that are constrained by observed trace gas concentrations. The prior land surface flux,
67 land surface observations, the meteorological inputs, and atmospheric transportation schemes are
68 all important for determining the accuracy of the modeled flux (Peters et al., 2007). As a result,
69 the deficiency in any of these four factors can limit the accuracy of the model.

70 In this study, we used several top-down approaches to evaluate the bottom-up fluxes of CO_2,
71 CH_4, and N_2O for a region dominated by agriculture. The inter-comparison of multiple
72 techniques was used to identify systematic biases of each method and constrain the overall
73 uncertainties. We first used CO_2 to evaluate the equilibrium boundary layer method against tall-
74 tower eddy covariance, flux aggregation, and the flux produced by an inverse model. We then
75 applied the equilibrium method to estimate the CH_4 and N_2O fluxes. The final task was to
76 compare the CH_4 and N_2O fluxes with two bottom-up emission inventories: 1) EDGAR42
77 (European Commission, Joint Research Centre [JRC]/Netherlands Environmental Assessment
78 Agency [PBL], Emission Database for Global Atmospheric Research [EDGAR], release version
79 4.2, http://edgar.jrc.ec.europa.eu, 2011), an inventory dataset used widely in atmospheric models
80 (Jeong et al., 2012); and 2) a national GHG inventory developed by the U.S. Environmental
81 Protection Agency (U.S. EPA, 2014).

82

2. Data and Methods

2.1 Research site

The boundary layer observations were made on a 244 m communication tower (KCMP tower) located at the Rosemount Research and Outreach Center, University of Minnesota, about 25 km south of Minneapolis/Saint Paul (44°41'19"N, 93°4'22"W). According to the U.S. Department of Agriculture Crop Data Layer data in 2009, the landscape around the tall tower was dominated by cropland, which accounted for 41% of the land cover within the 10 km radius of the tower and 37% within the 600 km radius. Corn and soybean were the dominant crop species, accounting for 55% and 38% of the cropland, respectively. About 40% of the land within the 600 km radius was covered by forest, grassland and pasture. The other land use was comprised of developed land, wetland, and open water. The land cover pattern described here for 2009 had a smaller corn to soybean ratio than that reported by Griffis et al. (2010) for 2007. This difference was mainly attributed to more corn plantation in 2007 stimulated by increased ethanol biofuel demand.

2.2 Mixing ratio data

CO_2 mixing ratios at the 32 m, 56 m, 100 m, and 200 m heights above the ground were measured by a tunable diode laser analyzer (TDL) (model TGA 100A, Campbell Scientific Inc., Logan, UT, USA) (Griffis et al., 2010). Air at these levels was drawn down by a pump (model DOA-V502A-FB, Gast Group Inc., Benton Harbor, MI, USA) through four Synflex tubes (6.25 mm ID) at a line pressure of 60 kPa and at a flow rate of 16 L min^{-1}. The air was sampled sequentially, each for 30 s. The sampled air was dried prior to analysis using a Nafion drier and brought to a common temperature. The CO_2 measurement was calibrated for every measurement cycle against the National Oceanic and Atmospheric Administration-Earth System Research

105 Laboratory (NOAA-ESRL) standards. The hourly precision of the CO_2 measurement was
106 approximately 0.03 ppm.

107 In addition, an intensive campaign was carried out from August 30 to September 25 (DOY 243 -
108 269), 2009. During this campaign, we measured CO_2, H_2O, CH_4, and N_2O mixing ratios at the
109 200 m and 3 m height on the tower. Air was drawn from these heights at a flow rate of 1.3 L min^{-1}
110 and 0.9 L min^{-1}, respectively, through two Synflex tubes (6.25 mm ID). A portion (0.6 L min^{-1})
111 of this flow was delivered to an infrared gas analyzer (IRGA model LI-6262, LI-COR, Lincoln,
112 NE, USA) for CO_2 and H_2O mixing ratio measurements, and a small amount (180 mL min^{-1}) was
113 delivered to another TDL for CH_4 and N_2O measurements. Measurement precisions for CO_2,
114 CH_4, and N_2O were 0.2 ppm, 1.2 ppb, and 0.5 ppb, respectively. The IRGA was manually
115 calibrated with a standard CO_2 gas (391.03 ± 0.03 ppm) and a dew point generator (LI-610, LI-
116 COR) at the beginning of the experiment. The accuracy of its measurement was improved in
117 post-field analysis by adding offsets so that its 200-m reading matched that registered by the
118 TDL CO_2 analyzer for the same height. The TDL for N_2O and CH_4 measurement was plumbed
119 to a four-port manifold that used a switching sequence in the order of 200 m, 3 m, calibration
120 zero and calibration span, with 30 s spent on each port and the first 15 s after each switching
121 omitted from the analysis. The N_2O concentration of the calibration span was traceable to a
122 NOAA-ESRL gold standard. The CH_4 concentration of the calibration span was calibrated
123 against a known standard provided by a local supplier and was also traceable to the NOAA-
124 ESRL standard scale.

125 **2.3 Eddy covariance data**

126 A closed-path EC system installed at the height of 100 m on the tower was used to measure the
127 CO_2 flux from 2007 to 2009 (Griffis et al., 2010). This system consisted of a 3-D sonic

anemometer-thermometer (model CSAT3, Campbell Scientific Inc.) and the TDL analyzer (model TGA 100A, Campbell Scientific) for CO_2 concentration. The sample tubing was 125 m long (6.25 mm ID, Synflex), which resulted in a typical lag time of 11 s, with Reynolds numbers exceeding 3500. Fluctuations in the velocities and concentrations were recorded at 10 Hz, and a block averaging time of 60-min was used to capture the dominant flux-containing frequencies.

Further, in 2009 two closed-path eddy covariance systems were used at two 10-m towers in the middle of corn (G21) and soybean fields (G19) (Baker and Griffis, 2005) about 3 km away from the tall tower. They recorded half-hourly fluxes of CO_2 and H_2O.

2.4 Top-down flux estimation methods

2.4.1 Tall-tower eddy covariance

Briefly, the tall-tower CO_2 flux was determined as the sum of the eddy covariance term measured at the 100-m height ($\overline{w'c'}$) and the storage term between the land surface and this height (F_S).

$$F_{EC} = \overline{w'c'} + F_S \quad (1)$$

Here, we assume that horizontal and vertical advection were negligible (Davis et al., 2003; Griffis et al., 2010). Wind statistics and fluxes were transformed into the planar fit coordinate system (Lee et al., 2004). Eddy fluxes were computed using the maximum covariance method with strict limits on window size based on manifold pressure and flow rates. Flux losses attributed to a combination of sensor separation, sonic path averaging, tube attenuation, and block averaging were estimated using the analytical model of Massman (2000). These losses typically ranged between 5% and 20%. A detailed description of the eddy covariance system and flux calculation can be found in Griffis et al. (2010).

The eddy covariance method does not perform well in stable atmospheric conditions and friction velocity ($u*$) is commonly used as a quality control for such conditions (Davis et al., 2003; Goulden et al., 1996). In this study, we discarded the nighttime flux data when $u*$ was less than 0.10 m s^{-1}, which is a threshold often used for agricultural environments (Baker and Griffis, 2005; Griffis et al., 2005).

Large negative fluxes in the early morning have been observed at many eddy covariance tower sites, and it may lead to an overestimation of CO_2 uptake during the growing season by as much as 20% (Anthoni et al., 1999; Davis et al., 2003; Yi et al., 2000). Davis et al. (2003) suggested that this bias is caused by horizontal and vertical advection, and it can be corrected by excluding the negative CO_2 flux that exceeds a pre-defined level. In this study, we excluded the morning (06:00 and 10:00 LST) data when the storage term was large (i.e. F_S < -4 μmol m^{-2} s^{-1}). This storage term screening reduced the estimated CO_2 uptake during the growing season (May to September) by 18% and is consistent with that reported in the literature (Davis et al., 2003; Yi et al., 2000). Details about the calculation of the storage term and a discussion about the data-screening standard for the negative storage term in early morning is reported in the supplementary materials (Section S1).

The monthly CO_2 flux was determined by the mean of the composite diurnal variation of the CO_2 flux. In 2009, excluding the malfunctioning of the instrumentation, the available data was 78%. The $u*$ and storage term screening eliminated an additional 12% and 2% of the data, respectively. We estimated the monthly mean from the diurnal composite of the CO_2 flux based on valid observations (Section S2 in supplementary materials).

171 **2.4.2 Equilibrium method**

172 The equilibrium method (EQ) provides a way to quantify regional trace gas fluxes from mixing
173 ratio measurements in the boundary layer (Bakwin et al., 2004; Betts, 2000; Betts et al., 2004;
174 Denmead et al., 1996; Desai, 2010; Helliker et al., 2004; Williams et al., 2011). So far, this
175 method has been applied to CO_2 and N_2O (Griffis et al., 2013) but not to CH_4. The EQ method
176 assumes that, over relatively long timescales (weeks), the diurnal dynamics of boundary layer
177 processes can be ignored and the boundary layer reaches statistical equilibrium (Griffis et al.,
178 2013; Helliker et al., 2004). Therefore, the averaged horizontal advection and storage are
179 negligible in the boundary layer budget (Williams et al., 2011) and the land surface flux (F_{Eq}) is
180 in balance with the exchange at the top of the boundary layer, as

181 $$\mathrm{F_{Eq}} = \rho \mathrm{W}(\mathrm{c_+} - \mathrm{c_m}) \quad (2)$$

182 where c_+ and c_m are the mixing ratio of CO_2, CH_4 or N_2O above and within the boundary layer,
183 respectively and ρ and W are air density and the vertical velocity, respectively, at the top of
184 boundary layer. Here c_+ was assumed as the concentration measured at Niwot Ridge (NWR,
185 40°3'11"N, 105°35'10"W) CO, USA, which is the closest background site operated by NOAA
186 (Conway et al., 1994) and is upwind of KCMP tower in the Ferrel cell. c_m was the concentration
187 at 200 m measured by TDL analyzers and calibrated to the NOAA-ESRL standards. The
188 concentrations used in the calculation were the composite diurnal variations for each month in
189 the case of CO_2 and the diurnal composites for the intensive campaign in the case of CH_4 and
190 N_2O. The equilibrium method was used for calculating the CO_2 flux from 2007 to 2009.
191 However, due to availability of data, the comparison among methods is limited to the 2009 CO_2
192 fluxes.

We used the following two methods to determine ρW (Helliker et al., 2004) for the three GHGs:

$$\rho W = \frac{F_w}{c_{w,+} - c_{w,m}} \quad (3)$$

$$\rho W = -\frac{\Omega}{g \cdot M_{air}} \quad (4)$$

where F_w and $c_{w,m}$ are the water vapor flux and mixing ratio measured at 100 m and 200 m on the tall tower, respectively, $c_{w,+}$, and Ω are the water vapor mixing ratio and the pressure vertical velocity (in units of Pa s^{-1}) at the 700 hPa level in the NCEP/NCAR Reanalysis-2 data, g is gravitational acceleration, and M_{air} is molecular mass of dry air (g mol^{-1}). ρW calculated from equation 3 is essentially the same as equation 4 under the EQ assumptions, because large scale synoptic subsidence dominates the exchange at the top of the boundary layer (Helliker et al., 2004). In addition, for CH_4 and N_2O, we also used CO_2 as a tracer to determine ρW:

$$\rho W = \frac{F_C}{c_{C,+} - c_{C,m}} \quad (5)$$

where F_C is the CO_2 flux measured by the EC system on the tall tower, $c_{C,+}$ and $c_{C,m}$ are the CO_2 mixing ratio measured at the NWR background site and at the 200 m level on the tall tower, respectively.

2.4.3 Inverse modeling

We used the CO_2 flux product from the global inversion model CarbonTracker 2011_oi (CT) (Peters et al., 2007 with updates documented at http://carbontracker.noaa.gov) as a reference to compare with the flux determined with the methods described above. This product provides three-hourly CO_2 fluxes from 2000-2010 at a spatial resolution of 1° by 1°, so the number of grid

points within the 100 km, 200 km, 300 km, and 600 km radii of the tall tower is 2, 10, 25, and 90, respectively.

The inversion CO_2 flux consists of fossil fuel burning, fire, land, and ocean flux. The CO_2 flux from fossil fuel was the average of two fossil fuel CO_2 emission datasets: one is the legacy CarbonTracker fossil fuel product using the global total from the Carbon Dioxide Information and Analysis Center (CDIAC, Boden et al. 2011) and the spatial distribution from EDGAR; and the other is the ODIAC (Open-source Data Inventory for Anthropogenic CO_2) emission product reported by Oda and Maksyutov (2011).

2.5 Flux aggregation (FA)

The regional trace gas flux (F_{FA}) can be estimated by aggregating sectorial and spatial fluxes using sectorial statistics and land cover information (Chen et al., 2008; Desai et al., 2008; Nisbet and Weiss, 2010; Tang et al., 2012). The total CO_2 flux from the landscape is the sum of the anthropogenic flux and biological flux. In this study, the anthropogenic flux (F_{ant}) was the prescribed fossil fuel flux in the CarbonTracker product for a target region. The biological flux was calculated by aggregating the CO_2 flux from six major land cover types.

$$\mathrm{F_{FA}} = \mathrm{F_{ant}} + \sum_{\mathrm{i=1}}^{6} \mathrm{frac_i} \cdot \mathrm{F_{bio,i}} \quad (6)$$

In this equation, $frac_i$ is the fraction of land cover type *i* for a target region, and $F_{bio,i}$ is the CO_2 flux from land cover type *i*. The six land cover types are cropland (corn and soybean), forest, grassland/pasture, wetland, open water, and developed land.

In order to compare with the fluxes from top-down methods, we estimated the bottom-up flux using the flux aggregation method within the tall tower footprint. Various methods have been developed for determining the footprint of the concentration or eddy flux measurement (Chen et

al., 2009; Kljun et al., 2004; Lin et al., 2003; Vesala et al., 2008). We used two footprint methods. The first method is based on determining an equally-weighted circular footprint centered at the tall tower. This method assumes that the area within each circular footprint has the same influence on the flux measured at the tall tower despite its distance from the tower, and therefore, $frac_i$ is the fraction of land cover type *i* within a certain radius around the tall tower. We tested the radii from 5 km to 600 km because the fetch of the EC flux footprint is thought to be 10 (during strong convection) to 100 (during neutral or stable condition) times the measurement height (Horst and Weil, 1992; Davis et al., 2003), however, some studies also suggest that the fetch-to-measurement-height ratio is much higher than 100 when the flux is measured at a high level (e.g. higher than 20 m) (Gash, 1986; Leclerc and Thurtell, 1990). The second footprint method we applied derives the footprint from the Stochastic Time-Inverted Lagrangian Transport model (STILT, Lin et al., 2003). During September, when the intensive campaign was carried out, we released 100 air parcels hourly at the tower and transported these parcels backward for two days. The distribution of the air parcels determined the tall tower footprint. (This footprint represents the source area of the EQ flux calculated based on the 200 m concentration.) Therefore, $frac_i$ was determined by overlaying the weighted footprint map with the land cover map. The values of $frac_i$ from these two different methods are summarized in Table S3 of the supplementary materials.

The cropland CO_2 flux was the weighted average of the flux measured with EC in a soybean field and a cornfield near the tall tower as described above. The forest CO_2 flux was obtained from the AmeriFlux data archive (Level 2 data) for the deciduous forest site at the University of Michigan Biological Station (UMBS), 662 km northeast of the tall tower (Curtis et al., 2005; Schmid et al., 2003). The grassland CO_2 flux was also from USIB2 AmeriFlux for Fermi Prairie,

Illinois, 503 km southeast of the tower (Gomez-Casanovas et al., 2012). Each of the three land cover types was measured by EC flux towers in 2009, and showed different seasonal patterns of CO_2 flux (Figure 1). The biological CO_2 flux from wetland, open water, and developed land was considered as negligible in this study, because these three land cover types only accounted for about 20% of the tall tower footprint, and the reported annual CO_2 fluxes from those land cover types were not significantly different from zero or relatively small (Striegl et al., 1998; Knoll et al., 2013; Olson et al., 2013). For example, Olson et al. (2013) reported that a temperate peat land in northern Minnesota, USA was a small net sink of CO_2 in 2009 (-26.8 ± 18.7 g C-CO_2 m^{-2} yr^{-1}), only about 5% of the CO_2 flux from a cornfield, and about 10% of the biogenic flux in the tall tower footprint. Considering the land fraction of peat land in the tall tower footprint, the CO_2 flux was estimated to be less than 1% of the biogenic flux.

3. Results

3.1 Constraints on the regional CO_2 flux

The tall tower EC CO_2 flux exhibits a strong seasonal pattern (Figure 2). From October to April, the landscape was a net source of CO_2, and the averaged efflux was 0.68 ± 0.10 μmol m^{-2} s^{-1} (the mean and standard deviation of the three annual values from 2007 to 2009). From May to September, the landscape was a sink of CO_2, reaching a peak uptake in July at the rate of -3.68 ± 0.99 μmol m^{-2} s^{-1}. There was no monthly mean data for June 2007 and June 2009 due to measurement problems. Since June is the only month that has missing CO_2 flux data for 2009, we gap-filled it according to the flux values observed in May to July 2008 and 2009. The annual cumulative flux in 2008 and 2009 was -24 and -131 g C-CO_2 m^{-2} yr^{-1}, respectively.

276 In order to test the size of the region that our monthly averaged EC flux represents, we first used
277 CT and FA methods to estimate the CO_2 flux with the equally-weighted circular footprint for a
278 radius up to 600 km and compared them with the EC flux. The monthly flux values from these
279 methods for the range of radii correlated well with the EC flux ($r > 0.9$, $p < 0.001$) (Table 1),
280 suggesting the land surface flux was relatively homogeneous and was dominated by the seasonal
281 pattern of the biological flux. Further, to test the accuracy of the estimation, the Nash-Sutcliffe
282 efficiency (NSE) was calculated (Nash and Sutcliffe, 1970), as

$$\mathrm{NSE} = 1 - \frac{\sum(o_i - m_i)^2}{\sum(o_i - \bar{o})^2} \tag{7}$$

283 where o_i is the EC flux and m_i is the regional mean flux from CT or FA. The summation is
284 performed over all months and the overbar denotes the mean over these months. It is considered
285 a very good fit when NSE > 0.75, and a good fit when 0.65 < NSE ≤ 0.75 (Moriasi et al., 2007).
286 The results show that the EC flux agrees very well with the regional mean flux from both the CT
287 and FA methods with a 200 km radius or larger (NSE > 0.80). Furthermore as the radius
288 increased from 200 km to 600 km, the CT and FA fluxes did not change significantly. The CT
289 and FA fluxes within a 100 km radius were more positive than the EC flux, mainly due to the
290 strong local anthropogenic emission from the Minneapolis/Saint Paul urban area. Consequently,
291 for the KCMP tower site, we can consider the EC flux as representing the average flux from 600
292 km radius around the tall tower, a typical size of the footprint of tall tower concentration
293 measurement (10^6 km^2; Gloor et al., 2001).

294 The aggregated flux based on the STILT footprint was -1.01μmol m^{-2} s^{-1} for the month of
295 September, 2009. In comparison, the EC flux during the same period was -0.93 μmol m^{-2} s^{-1}, and
296 the FA flux with a 300 km and 600 km radius was -1.04 μmol m^{-2} s^{-1} and -0.94 μmol m^{-2} s^{-1},

297 respectively. The results again confirm that the land cover type around the tower was relatively
298 homogeneous at scales ranging from 200 to 600 km.

299 Consequently, we consider the tall-tower EC flux as a robust estimate of the regional flux and
300 used it to evaluate the performance of the EQ method. Two CO_2 fluxes were determined by EQ
301 method for each month, one using H_2O as a tracer (F_{EH}, calculated with ρW with Eq 3) and the
302 other using ρW in the NCEP reanalysis data (F_{EO}, calculated with ρW with Eq 4) (Figure 3).
303 Both F_{EH} and F_{EO} reproduced the seasonal pattern of the EC flux ($r > 0.85$, $p < 0.001$) but
304 significantly underestimated the magnitude of the flux in July. The F_{EH} and F_{EO} fluxes were only
305 31% and 48% of the EC flux in July.

306 **3.2 GHG concentration patterns**

307 During the intensive campaign, the CO_2 mixing ratio at the height of 200 m increased from 365.2
308 ppm during the first five days to 406.2 ppm during the last five days (Figure 4). The mixing ratio
309 changed from below that at the NWR (384.4 ppm) to above that at the NWR site, indicating a
310 transition of the landscape from a CO_2 sink to a source. This observation is consistent with the
311 seasonal pattern in the CO_2 flux shown in Figure 3.

312 The mean CH_4 mixing ratio during the observation period was 2.096 and 2.017 ppm at the
313 heights of 3 m and 200 m, respectively. The CH_4 mixing ratio at both heights was consistently
314 higher than the background mixing ratio at NWR (1.844 ppm), suggesting that the landscape
315 around the tall tower was a CH_4 source.

316 The N_2O mixing ratio during the observation period was also higher than that at NWR. The
317 average N_2O mixing ratio at the heights of 3 m and 200 m was 326.7 and 324.8 ppb, which were

4.0 ppb and 2.1 ppb higher than the value at NWR site (322.7 ppb), respectively, indicating that the landscape was a N_2O source during the observation period.

3.3 Regional CH_4 and N_2O fluxes

We applied the EQ method in estimating the regional CH_4 and N_2O fluxes during the intensive campaign. During this period ρW determined with three independent methods (using CO_2 and H_2O tracers and the NCEP reanalysis data) was -0.09 ± 0.02 mol m^{-2} s^{-1} (mean ± 1 standard deviation of the three estimates) The CH_4 and N_2O fluxes were 16.0 ± 3.1 nmol m^{-2} s^{-1} and 0.19 ± 0.04 nmol m^{-2} s^{-1}, respectively.

In order to estimate an annual budget of CH_4 and N_2O with the EQ method, we need the CH_4 and N_2O mixing ratio within and above the boundary layer for the whole year. Therefore, we assumed that the seasonal pattern of the CH_4 and N_2O mixing ratios at the KCMP tower was identical to the pattern at a nearby NOAA tall tower site (WBI in Iowa) (Andrews et al., 2013a; Andrews et al., 2013b; Dlugokencky et al., 2013), and extrapolated the CH_4 and N_2O concentration during the intensive campaign period to the whole year for 2009 according to the seasonal pattern at the WBI site. The WBI site was chosen because it has similar land cover types in its footprint as the KCMP tower site (Zhang et al., 2014). The CH_4 and N_2O mixing ratios above the boundary layer were determined at the NWR site and ρW were determined by the three methods (Equation 3-5) throughout the year 2009 (Figure S6). It follows that the annual regional CH_4 and N_2O fluxes were 22.4 ± 4.2 nmol m^{-2} s^{-1} and 0.49 ± 0.09 nmol m^{-2} s^{-1}, respectively. The uncertainties of the annual fluxes were the result of the uncertainties in ρW. In comparison, the annual CH_4 and N_2O fluxes at the WBI tower were 14.5 nmol m^{-2} s^{-1} and 0.32 nmol m^{-2} s^{-1} using the EQ method (Zhang, 2013). The impact of advection was considered as negligible since there was no prevailing wind direction throughout the year of 2009.

4. Discussion

4.1 Annual carbon dioxide flux

Determining the annual CO_2 flux at the regional scale is challenging because the flux has both diurnal and seasonal cycles and the magnitude of the annual average is substantially smaller than the seasonal and diurnal variations. For example, in 2009, the tall tower's annual average EC flux was -0.35 μmol m^{-2} s^{-1} (-131 g C-CO_2 m^{-2} yr^{-1}), while the seasonal variation was about 6 μmol m^{-2} s^{-1} and the diurnal variation during summer time was about 40 μmol m^{-2} s^{-1}, about 16 and 113 times, respectively, higher than the annual average. So far, there is no single method that can directly assess the regional CO_2 flux, because for all the available methods there are periods or conditions where the underlying theory is not met or where the available data is limited to truly capture the temporal and spatial variability. A small systematic bias in the daily and monthly flux estimation, such as that caused by the data-screening and gap-filling approaches, is significant for the annual average CO_2 flux, and it may result in opposite conclusions of whether the landscape is a carbon source or a sink.

A number of studies have attempted to estimate the annual CO_2 flux in the vicinity of the Upper Midwest USA (Table 2) (Davis et al., 2003; Bakwin et al., 2004; Helliker et al., 2004; Ricciuto et al., 2008). Based on EC measurements on the LEF tall tower, which is about 260 km northeast of the KCMP tower, Ricciuto et al. (2008) reported that the annual CO_2 flux was 120 g C-CO_2 m^{-2} yr^{-1} with a strong inter-annual variation from 1997 to 2004 (140 g C-CO_2 m^{-2} yr^{-1}). This result was similar to Davis et al.'s (2003) result, but opposite to Helliker et al.'s (2004) EC flux for 2000, the latter of which is -71 g C-CO_2 m^{-2} yr^{-1}. The major difference is that Helliker et al. (2004) did not gap-fill the data, and the reported CO_2 flux has excluded the periods when water vapor flux was not available.

Our annual CO_2 flux was calculated as the average of monthly fluxes, and the monthly fluxes were determined by the diurnal composite of available observations after u_* and storage term screening. We performed a Monte Carlo simulation to assess the uncertainty associated with missing data following Griffis et al. (2003). We randomly removed 30% of the data for each month, and recorded the calculated monthly and annual fluxes following the same data processing procedure. By repeating this simulation 5000 times, we determined the standard deviation of the annual flux estimates. As a result, the uncertainty in the annual CO_2 flux due to data gaps was ± 31 g C m^{-2} yr^{-1}. In addition, the random errors in hourly averaged EC flux may also significantly affect the annual budget. Assuming a 20% random error in hourly EC flux, the resulting uncertainties in annual flux was ± 4 g C m^{-2} yr^{-1}, about one magnitude lower than the uncertainties from data gaps (Morgenstern et al., 2004). Considering the uncertainties from data gaps and random errors, the 2009 CO_2 budget was -131± 35 g C m^{-2} yr^{-1}, suggesting the region around the tall tower was a carbon sink.

The uncertainty of the annual FA estimate was affected by the accuracy of the land cover information, the carbon flux data for each land cover type, and anthropogenic emissions. We assessed the uncertainties of the annual CO_2 flux from each land cover type with the method used for tall tower EC flux (Table 2), and assume the uncertainty of anthropogenic emission was 10% (NRC, 2010). Without considering the uncertainties in land cover information, the annual FA flux was -130 ± 13 g C m^{-2} yr^{-1}. The accuracy of the Crop Data Layer was 85%-95% for major crops (Boryan et al., 2011), therefore, we assume that the fraction of each land cover type has an uncertainty up to 20%. By using a Monte Carlo simulation we estimated the uncertainty of the annual FA estimate will increase to 34 g C m^{-2}. In other words, the FA annual flux (-130 ± 34 g C-CO_2 m^{-2} yr^{-1}) showed very good agreement with the EC flux in 2009.

Although the CT monthly flux tracked the seasonal pattern of the EC and FA flux, the annual CT flux was -54 g C-CO_2 m^{-2} yr^{-1}, considerably lower than EC and FA annual fluxes. This indicates that the CT method performed reasonably well on reproducing the monthly fluxes, but that it systematically underestimated the annual flux compared to the other methods.

Overall, the good agreement between EC (a top-down method) and FA (a bottom-up method) provides strong evidence that the landscape around the tall tower was a carbon sink at the rate of -131± 35 g C m^{-2} yr^{-1} in 2009.

4.2 Uncertainties in CO_2 flux from the equilibrium method

The EQ method provided good estimates of the CO_2 flux for each month except July, when the regional CO_2 flux was the most negative (strong sink) during 2009. Excluding July, the difference between the monthly EC flux and EQ flux in 2009 was 0.37 ± 0.29 μmol m^{-2} s^{-1}, only 6% of the seasonal variation (6 μmol m^{-2} s^{-1}).

The underestimation of the EQ flux might be attributed to uncertainties in ρW or concentration difference at the top of boundary layer ($c_+ - c_m$), according to Equation 2. In July, the ρW was -0.17 mol m^{-2} s^{-1} (Eq 3) and -0.26 mol m^{-2} s^{-1} (Eq 4) while the concentration difference was 9.03 ppm. To bring the equilibrium flux into agreement with the tall-tower EC flux (-4.82 μmol m^{-2} s^{-1} in July 2009), ρW would have to increase to -0.53 mol m^{-2} s^{-1}, which is much larger in magnitude than -0.26 ± 0.09 mol m^{-2} s^{-1}, the average July value for 2007 to 2011 obtained with the NCEP reanalysis data. The 0.09 mol m^{-2} s^{-1} uncertainty in ρW (the standard deviation of July ρW from 2007 to 2011) leads to 0.81 μmol m^{-2} s^{-1} uncertainty in the monthly flux, about 17% of the July flux. In addition, the monthly ρW values in 2007 to 2011 period were mostly within -0.18 ± 0.08 mol m^{-2} s^{-1}, and the maximum and minimum values were -0.05 and -0.36 mol m^{-2} s^{-1}.

409 Even the most negative value in the five-year period cannot fully explain the underestimation of
410 the EQ flux in July, indicating that the concentration difference at the top of boundary layer may
411 be underestimated.

412 Two sources of uncertainty exist in the concentration difference observed at the top of boundary
413 layer ($c_+ - c_m$). One is the accuracy of the CO_2 measurement at 200 m level of the KCMP tower
414 site and NWR background site, and the other is the assumption that those two concentrations are
415 the same as the concentration within and above the boundary layer. The CO_2 concentration at the
416 KCMP tower was calibrated with the NOAA-ESRL standard throughout the measurement, and
417 the measurement precision was 0.03 ppm. Meanwhile, the precision at NWR site was on the
418 order of 0.1 ppm (Helliker et al., 2004). As a result the first source of uncertainty led to about
419 0.04 μmol m^{-2} s^{-1} uncertainties, which was not significant.

420 The second source of uncertainty can potentially lead to 1.55 μmol m^{-2} s^{-1} uncertainties in the
421 July CO_2 flux. Even though the NWR site is only about 5^o south of the KCMP tower, CO_2
422 concentration at the NWR site may be significantly different from the CO_2 concentration above
423 the boundary layer at the KCMP site, due to a large latitudinal CO_2 gradient (Denning et al.,
424 1995). To examine the uncertainties in using CO_2 concentration at NWR site as a proxy for c_+
425 we surveyed the following observation data that could be used as a proxy for c_+ in July 2009: 1)
426 the CO_2 concentration in the Marine Boundary Layer at the same latitude as the KCMP tower
427 was 382.47 ppm; 2) the average CO_2 concentration measured by aircraft (between 3000 m-4500
428 m) at three sites near the KCMP tower were 384.80 ± 4.55 ppm (Cooperative Global
429 Atmospheric Data Integration Project, 2014; Yi et al., 2004); 3) the average CO_2 concentrations
430 in the nearby background sites were 380.03 ppm (Cold Bay, Alaska, US) and 383.81 ppm
431 (Barrow, Alaska, US). The CO_2 concentration at the NWR site (386.01 ppm) is not significantly

different from the aircraft measurements and is lower than the rest of the concentrations with the maximum difference of 5.98 ppm. Therefore, the CO_2 concentration at NWR site may overestimate c_+ by up to 5.98 ppm and result in up to 1.55 μmol m^{-2} s^{-1} uncertainty in the July CO_2 flux. The uncertainties in other months in 2009 were examined and presented in the supplementary materials (Section S4).

Bakwin et al. (2004) adjusted the CO_2 concentration at the 30 m height by increasing it by 2.5 ppm to estimate c_m in the summer. Since our CO_2 concentration was measured at 200 m, a much higher level, the uncertainty in using 200 m concentration to estimate c_m should be much less than 2.5 ppm. Direct measurement at the top of the boundary layer is needed to evaluate these two important uncertainties.

Another more likely source for the significant underestimation in July is that horizontal advection is not negligible when the prevailing winds align with a strong spatial CO_2 gradient. With a tall tower observation network, Miles et al. (2012) reported that the CO_2 gradients between the KCMP tower and other sites range from 0.3 to 2.1 ppm 100 km^{-1} during the growing season. The CarbonTracker 3-D CO_2 concentration product also shows large CO_2 depletion in the upper Midwest Corn Belt during the growing season due to the strong CO_2 uptake by corn plants. According to this product, the mean concentration of the 34 m – 1274 m air layer has an averaged gradient of 0.8 ppm / (100 km) along the prevailing wind (from northwest) in July 2009 (Figure 5). Using a mean wind speed of 5.4 m s^{-1} recorded on the tall tower and a boundary layer depth of 1000 m (Yi et al., 2001), the resulting advection flux was -1.88 μmol m^{-2} s^{-1}, which is comparable to the bias of the equilibrium method. In comparison, the EC flux was not as sensitive to the advective influence. For instance, using the same spatial gradient data, the

advection flux at the 100 m level was only -0.02 μmol m^{-2} s^{-1} according to the accumulated concentration for the lowest two grid levels in the CarbonTracker product (34.5 m and 112 m).

Overall, the uncertainties in ρW, $(c_+ - c_m)$, and horizontal advection can potentially lead to uncertainties in the July CO_2 flux estimate on the order of 0.81, 1.55, and -1.88 μmol m^{-2} s^{-1} respectively, and they might be large enough to account for the discrepancy between EQ and EC methods for July 2009 and the annual 2009 flux. Direct and accurate measurements of these three terms using methods such as aircraft (Yi et al., 2004) or drones are needed to reduce these uncertainties.

4.3 Uncertainties in the CH_4 and N_2O fluxes

Uncertainties in trace gas concentration measurements within and above the boundary layer can lead to large uncertainties in the trace gas flux estimation. The averaged CH_4 concentrations during the intensive campaign at the nearby background sites were 1.883 ppm (Cold Bay, Alaska, US), 1.887ppm (Barrow, Alaska, US), and 1.842 ppm (NWR, Colorado, US). The maximum difference between NWR and the other background sites in North America was 0.045 ppm. If the measurements at these other sites were used for the concentration above the boundary layer at the tall tower site, the regional flux would decrease by up to 4.1 nmol m^{-2} s^{-1}, or about 30% of the estimated EQ flux. In addition, the uncertainty in our CH_4 concentration measurement caused by uncertainties in the calibration standard was 0.055 ppm, with a resulting uncertainty in the flux of ± 5.0 nmol m^{-2} s^{-1}. The combined uncertainty range of the CH_4 flux is 6.9-21.0 nmol m^{-2} s^{-1}.

The systematic bias in the trace gas measurement between the KCMP tower and NOAA background sites was avoided in the other two independent boundary layer methods, which

476 depend on the relative concentration difference at 3 m and 200 m levels and the build-up (change
477 in concentration with time) concentration at night. Here, we used these two methods, a modified
478 Bowen ratio method (Werner et al., 2003) and a modified nocturnal boundary layer method
479 (Kelliher et al., 2002), to calculate the nighttime CH_4 flux for comparison with the equilibrium
480 estimate. The modified Bowen ratio method assumes that the vertical transport of a trace gas is
481 driven by eddy diffusion and that the diffusivity is the same for all scalar quantities. The
482 nocturnal boundary layer method uses CO_2 as a tracer and assumes that the build-up of CO_2 and
483 CH_4 near the land surface is caused by land surface emissions. The CH_4 fluxes from these two
484 methods were 14.8 ± 10.3 nmol m^{-2} s^{-1} and 17.1 ± 9.4 nmol m^{-2} s^{-1} (Zhang et al., 2013),
485 respectively. The results confirm that the CH_4 flux from the equilibrium method (16.0 nmol m^{-2}
486 s^{-1}) gave a reasonable estimation of the regional flux.

487 N_2O has a much more homogeneous background concentration than CH_4 and CO_2. The
488 differences between the background sites in the northern hemisphere were less than 0.5 ppb
489 during the intensive campaign. The N_2O measurements at the tall tower were calibrated against
490 NOAA-ESRL standards and, therefore, can be compared against the NOAA background sites.
491 The uncertainties in the background concentration will lead to a bias within 0.05 nmol m^{-2} s^{-1} for
492 the N_2O flux estimation, or 26% of the estimated N_2O flux (0.19 nmol m^{-2} s^{-1}). Applying the
493 modified Bowen ratio method and the modified nocturnal boundary layer method, we obtained a
494 regional nighttime N_2O flux of 1.09 ± 0.56 nmol m^{-2} s^{-1} and 0.90 ± 0.65 nmol m^{-2} s^{-1},
495 respectively, both of which were higher than the flux estimated from the equilibrium method. It
496 is possible that EQ method underestimated the regional N_2O flux because the advection was not
497 negligible during the intensive observation period, but it is not feasible to evaluate due to scarce
498 N_2O concentration measurements.

4.4 Climate impact of the major GHG fluxes

According to the KCMP tower measurement, the regional fluxes of three major greenhouse gases in 2009 were -131 ± 35 g C-CO_2 m^{-2} yr^{-1}, 8.50 ± 1.58 g C-CH_4 m^{-2} yr^{-1}, and 0.43 ± 0.08 N-N_2O m^{-2} yr^{-1}. The global warming potential (GWP) over a 100-year time horizon for CO_2, CH_4, and N_2O was -480 ± 128, 283 ± 53, and 205 ± 37 g CO_2 eq m^{-2} yr^{-1} respectively. The GWP for CO_2 was a result of anthropogenic emission (454 g CO_2 eq m^{-2} yr^{-1}, according to the fossil fuel emission prescribed in CarbonTracker product) and biological CO_2 uptake (934 g CO_2 eq m^{-2} yr^{-1}) for the region around the tall tower (Table 2). The total climate impact of the CH_4 and N_2O emission offset about 30% and 22% of the biological CO_2 uptake and was comparable to the anthropogenic CO_2 emission, indicating the important role of CH_4 and N_2O for the regional GHG emission portfolio.

Considering all three major GHG fluxes, the landscape around the tall tower had a near neutral impact on the climate in 2009 (7 ± 160 g CO_2 eq m^{-2} yr^{-1}). This conclusion, however, did not consider that the carbon fixed by crops will be harvested and some fraction will be transported and emitted outside of the tall tower footprint. According to West et al. (2011), the harvested biomass from the KCMP tower footprint is approximately 140 g C m^{-2} yr^{-1} (513 g CO_2 eq m^{-2} yr^{-1}). In other words, the tall tower footprint likely has a warming impact on the climate when all three major GHG fluxes and emission leakage (i.e. loss of carbon to the atmosphere from harvested biomass) are considered.

4.5 Comparison with bottom-up inventories

EDGAR is a widely used anthropogenic GHG inventory for atmospheric research, having fine spatial resolutions (0.1° × 0.1°) (Jeong et al., 2012; Zhao et al., 2009). So far, only a few studies have evaluated it with atmospheric observations. These studies indicate that EDGAR may have

522 significantly underestimate N_2O and CH_4 emission in North America by as much as three times
523 (Kort et al., 2008; Miller et al., 2012).

524 We first compared the CH_4 and N_2O fluxes at the KCMP tower during the intensive campaign
525 with EDGAR42 for the area within the 300 km radius around the tower, and found that the CH_4
526 flux was 5.8 times higher and the N_2O flux was 50% higher than the EDGAR42 values. In this
527 comparison, the EDGAR42 annual estimate was scaled to the emissions in September using its
528 seasonal factor (1.1 for September). Another comparison was carried out on the annual time
529 scale. The estimates of the annual CH_4 and N_2O fluxes based on the tall tower EQ measurement
530 were 6-9 times and 2-3 times higher than the EDGAR42 annual flux respectively.

531 The primary reason for the lower regional CH_4 flux from EDGAR42 is because it has excluded
532 natural sources of CH_4. Wetland is the major natural CH_4 source in this region. Although
533 wetlands account for less than 5% of the land around the tall tower, it is not negligible in the
534 regional CH_4 budgeting because CH_4 emissions from wetlands can be as high as 250 nmol m^{-2} s^{-1}
535 in September (Bridgham et al., 2006). EDGAR42 may have also underestimated the CH_4
536 emission from anthropogenic sources, because it does not account for factors such as natural gas
537 leakage, and have low biases for the CH_4 emissions from agricultural activities (Mays et al.,
538 2009; Wunch et al., 2009; Ussiri et al., 2009).

539 We hypothesize that the lower N_2O flux in the EDGAR42 inventory is likely a result of the
540 underestimation of anthropogenic N_2O emission, since natural sources were not significant in the
541 region around the tall tower. A recent study on global N_2O emission from a natural ecosystems
542 suggests soil emissions in the upper-Midwest US is mostly around 0.10 kg N ha^{-1} yr^{-1} (0.01 nmol
543 m^{-2} s^{-1}) (Zhuang et al., 2012), only 10% of the EDGAR42 anthropogenic emission.

544 In addition to EDGAR42, we compare the CH_4 and N_2O fluxes measured at the KCMP tower
545 with the GHG inventory developed by the EPA (EPA inventory), which was based on more
546 country-specific emission factors or models (e.g. N_2O from agriculture soil was simulated with a
547 biogeochemical model). The national CH_4 and N_2O emissions in EPA inventory were 12% and 35%
548 higher than the EDGAR42 inventory. However, we cannot directly compare the EPA inventory
549 with the top-down estimates for a region since the EPA inventory does not have spatial
550 distribution for all emission sectors. If we assume that the spatial distribution of the EPA
551 inventory is the same as the EDGAR42 inventory, the EPA inventory brings the bottom-up
552 estimates closer to the top-down EQ estimates. But the tall tower EQ estimates for regional CH_4
553 and N_2O emissions were still 5-8 times and 1-2 times higher than the EPA inventory.

554 **5. Conclusions**

555 The regional budget of CO_2, CH_4, and N_2O for the Upper Midwest, USA was quantified with
556 multiple top-down and bottom-up approaches. The four methods for the regional CO_2 flux (tall-
557 tower eddy covariance, CarbonTracker inverse modeling, flux aggregation, and the equilibrium
558 boundary layer method) produced similar seasonal patterns (linear correlation of the monthly
559 flux > 0.85, $p < 0.001$). However, discrepancies exist in the magnitude of the monthly and annual
560 fluxes. The CarbonTracker annual flux for 2009 (-54 g C-CO_2 m^{-2} yr^{-1}) was much lower in
561 magnitude than the flux aggregation estimate (- 130 ± 37 g C-CO_2 m^{-2} yr^{-1}) and that measured
562 with eddy covariance (-131 ± 40 g C-CO_2 m^{-2} yr^{-1}). The equilibrium method significantly
563 underestimated the July uptake by 52-69% in comparison to eddy covariance. The
564 underestimation cannot be fully explained by the bias in ρW or concentration difference at the
565 top of the boundary layer, and we suggest that the large spatial gradient along the prevailing
566 wind in July 2009 was a main contributor to the underestimation.

The CH_4 and N_2O regional fluxes estimated from equilibrium method during the intensive campaign (DOY 243 – 269, 2009) were 16.0 ± 3.1 and 0.19 ± 0.04 nmol m^{-2} s^{-1}, respectively, and were 5.8 times and 50% higher than in the EDGAR42 inventory. The annual CH_4 and N_2O fluxes also suggest significant underestimation by the EDGAR42 inventory and the EPA inventory.

Considering the global warming potential on a 100-year time scale, the CH_4 and N_2O emissions from the landscape were comparable to the anthropogenic CO_2. The landscape appeared to have a near neutral impact on climate when all three major GHGs were considered. Our results confirm that for this agriculture dominated landscape, climate change mitigation should include CH_4 and N_2O emissions.

Acknowledgement

We would like to thank the University of Minnesota UMore Park for use of the facilities, and Matt Erickson (Department of Soil, Water, and Climate, University of Minnesota) for providing technical support for the tall tower measurement. Funding was provided by USDA NIFA/2010-65112-20528, the Yale Institute for Biospheric Studies, and the Yale Center for Environmental Law & Policy Research Prize Fellowship. Measurements at the WBI tower were funded by NOAA's Climate Program Office and are part of NOAA's contributions to the North American Carbon Program. We thank Professor Charles Stanier from the University of Iowa and his students for supporting the NOAA PFP measurements at the WBI tower. CarbonTracker CT2011_oi results provided by NOAA ESRL, Boulder, Colorado, USA from the website at http://carbontracker.noaa.gov.

References

Andrews, A. E., Kofler, J. D., Trudeau, M. E., Williams, J. C., Neff, D. H., Masarie, K. A., Chao, D. Y., Kitzis, D. R., Novelli, P. C., Zhao, C. L., Dlugokencky, E. J., Lang, P. M., Crotwell, M. J., Fischer, M. L., Parker, M. J., Lee, J. T., Baumann, D. D., Desai, A. R., Stanier, C. O., de Wekker, S. F. J., Wolfe, D. E., Munger, J. W., and Tans, P. P.: CO_2, CO and CH_4 measurements from the NOAA Earth System Research Laboratory's Tall Tower Greenhouse Gas Observing Network: instrumentation, uncertainty analysis and recommendations for future high-accuracy greenhouse gas monitoring efforts, Atmos. Meas. Tech. Discuss., 6, 1461-1553, doi:10.5194/amtd-6-1461-2013, 2013a.

Andrews, A.E., Lang, P.M., Crotwell, A.J., Kofler,J.D.: Nitrous Oxide Dry Air Mole Fractions from the NOAA ESRL Tall Tower Network using Programmable Flask Packages (PFP), Version: 2012-09-21, 2013b.

Anthoni, P. M., Law, B. E., and Unsworth, M. H.: Carbon and water vapor exchange of an open-canopied ponderosa pine ecosystem, Agric. For. Meteorol., 95, 151-168, doi:10.1016/s0168-1923(99)00029-5, 1999.

Baker, J. M., and Griffis, T. J.: Examining strategies to improve the carbon balance of corn/soybean agriculture using eddy covariance and mass balance techniques, Agric. For. Meteorol., 128, 163-177, doi:10.1016/j.agrformet.2004.11.005, 2005.

Bakwin, P. S., Davis, K. J., Yi, C., Wofsy, S. C., Munger, J. W., Haszpra, L., and Barcza, Z.: Regional carbon dioxide fluxes from mixing ratio data, Tellus Series B-Chemical and Physical Meteorology, 56, 301-311, doi:10.1111/j.1600-0889.2004.00111.x, 2004.

Betts, A. K.: Idealized model for equilibrium boundary layer over land, J Hydrometeorol, 1, 507-523, doi:10.1175/1525-7541(2000)001<0507:Imfebl>2.0.Co;2, 2000.

Betts, A. K., Helliker, B., and Berry, J.: Coupling between CO_2, water vapor, temperature, and radon and their fluxes in an idealized equilibrium boundary layer over land, Journal of Geophysical Research-Atmospheres, 109, Artn D18103, doi:10.1029/2003jd004420, 2004.

Boden, T.A., Marland, G., and Andres, R.J.: Global, Regional, and National Fossil-Fuel CO_2 Emissions. Carbon Dioxide Information Analysis Center, Oak Ridge National Laboratory, U.S. Department of Energy, Oak Ridge, Tenn., U.S.A., doi 10.3334/CDIAC/00001_V2011, 2011.

Boryan, C., Yang, Z. W., Mueller, R., and Craig, M.: Monitoring US agriculture: the US Department of Agriculture, National Agricultural Statistics Service, Cropland Data Layer Program, Geocarto Int, 26, 341-358, doi:10.1080/10106049.2011.562309, 2011.

Bridgham, S. D., Megonigal, J. P., Keller, J. K., Bliss, N. B., and Trettin, C.: The carbon balance of North American wetlands, Wetlands, 26, 889-916, doi:10.1672/0277-5212(2006)26[889:Tcbona]2.0.Co;2, 2006.

Chen, B. Z., Black, T. A., Coops, N. C., Hilker, T., Trofymow, J. A., and Morgenstern, K.: Assessing Tower Flux Footprint Climatology and Scaling Between Remotely Sensed and Eddy Covariance Measurements, Bound-Lay. Meteorol., 130, (2), 137-167, 2009.

Chen, B., Chen, J. M., Mo, G., Black, A., and Worthy, D. E. J.: Comparison of regional carbon flux estimates from CO(2) concentration measurements and remote sensing based footprint integration, Global Biogeochemical Cycles, 22, doi:10.1029/2007gb003024, 2008.

Conway, T. J., Tans, P. P., Waterman, L. S., and Thoning, K. W.: Evidence for Interannual Variability of the Carbon-Cycle from the National-Oceanic-and-Atmospheric-Administration Climate-Monitoring-and-Diagnostics-Laboratory Global-Air-Sampling-Network, Journal of Geophysical Research-Atmospheres, 99, 22831-22855, doi:10.1029/94jd01951, 1994.

Cooperative Global Atmospheric Data Integration Project: Multi- laboratory compilation of atmospheric carbon dioxide data for the period 2000-2013 (obspack_co2_1_CARBONTRACKER_CT2013_2014-05-08). Compiled by NOAA Global Monitoring Division: Boulder, Colorado, U.S.A. Data product accessed at http://www.esrl.noaa.gov/gmd/ccgg/obspack/, 2014.

Curtis, P. S., Vogel, C. S., Gough, C. M., Schmid, H. P., Su, H. B., and Bovard, B. D.: Respiratory carbon losses and the carbon-use efficiency of a northern hardwood forest, 1999-2003, New Phytol, 167, 437-455, doi:10.1111/j.1469-8137.2005.01438.x, 2005.

Davis, K. J., Bakwin, P. S., Yi, C. X., Berger, B. W., Zhao, C. L., Teclaw, R. M., and Isebrands, J. G.: The annual cycles of CO_2 and H_2O exchange over a northern mixed forest as observed from a very tall tower, Global Change Biol, 9, 1278-1293, doi:10.1046/j.1365-2486.2003.00672.x, 2003.

Denmead, O. T., Raupach, M. R., Dunin, F. X., Cleugh, H. A., and Leuning, R.: Boundary layer budgets for regional estimates of scalar fluxes, Global Change Biol, 2, 255-264, doi:10.1111/j.1365-2486.1996.tb00077.x, 1996.

Desai, A., Wang, W. G., and Cook, B. D.: Uncovering mechanisms of episodic methane sources observed by a very tall eddy covariance tower, 30th Conference on Agric. For. Meteorol./1st Conference on Atmospheric Biogeosciences, Boston, MA, U.S., 2012.

Desai, A. R., Noormets, A., Bolstad, P. V., Chen, J. Q., Cook, B. D., Davis, K. J., Euskirchen, E. S., Gough, C. M., Martin, J. G., Ricciuto, D. M., Schmid, H. P., Tang, J. W., and Wang, W. G.: Influence of vegetation and seasonal forcing on carbon dioxide fluxes across the Upper Midwest, USA: Implications for regional scaling, Agric. For. Meteorol., 148, 288-308, doi:10.1016/j.agrformet.2007.08.001, 2008.

Desai, A. R.: Climatic and phenological controls on coherent regional interannual variability of carbon dioxide flux in a heterogeneous landscape, Journal of Geophysical Research-Biogeosciences, 115, doi:10.1029/2010jg001423, 2010.

Desai, A. R., Helliker, B. R., Moorcroft, P. R., Andrews, A. E., and Berry, J. A.: Climatic controls of interannual variability in regional carbon fluxes from top-down and bottom-up perspectives, Journal of Geophysical Research-Biogeosciences, 115, doi:10.1029/2009jg001122, 2010.

667 Denning, A.S., Fung, I.Y., and Randall, D.A.: Latitudinal gradient of atmospheric CO_2 due to
668 seasonal exchange with land biota, Nature, 376, 240–243, 1995.
669 Dlugokencky, E., Lang, P.M., Crotwell, A.J.: Nitrous Oxide Dry Air Mole Fractions from the
670 NOAA ESRL Global Cooperative Air Sampling Network, Version: 2012-09-21, 2013.
671 Gash, J. H. C.: A Note on Estimating the Effect of a Limited Fetch on Micrometeorological
672 Evaporation Measurements, Bound-Lay Meteorol, 35, 409-413, doi:10.1007/Bf00118567,
673 1986.
674 Gloor, M., Bakwin, P., Hurst, D., Lock, L., Draxler, R., and Tans, P.: What is the concentration
675 footprint of a tall tower?, Journal of Geophysical Research-Atmospheres, 106, 17831-
676 17840, doi:10.1029/2001jd900021, 2001.
677 Gomez-Casanovas, N., Matamala, R., Cook, D. R., and Gonzalez-Meler, M. A.: Net ecosystem
678 exchange modifies the relationship between the autotrophic and heterotrophic components
679 of soil respiration with abiotic factors in prairie grasslands, Global Change Biol, 18, 2532-
680 2545, doi:10.1111/J.1365-2486.2012.02721.X, 2012.
681 Goulden, M. L., Munger, J. W., Fan, S. M., Daube, B. C., and Wofsy, S. C.: Measurements of
682 carbon sequestration by long-term eddy covariance: Methods and a critical evaluation of
683 accuracy, Global Change Biol, 2, 169-182, doi:10.1111/j.1365-2486.1996.tb00070.x, 1996.
684 Griffis, T. J., Black, T. A., Morgenstern, K., Barr, A. G., Nesic, Z., Drewitt, G. B., Gaumont-
685 Guay, D., and McCaughey, J. H.: Ecophysiological controls on the carbon balances of
686 three southern boreal forests, Agric. For. Meteorol., 117, 53-71, doi:10.1016/s0168-
687 1923(03)00023-6, 2003.
688 Griffis, T. J., Lee, X., Baker, J. M., Sargent, S. D., and King, J. Y.: Feasibility of quantifying
689 ecosystem-atmosphere (COO)-O-18-O-16 exchange using laser spectroscopy and the flux-
690 gradient method, Agric. For. Meteorol., 135, 44-60, doi:10.1016/j.agrformet.2005.10.002,
691 2005.
692 Griffis, T. J., Baker, J. M., Sargent, S. D., Erickson, M., Corcoran, J., Chen, M., and Billmark, K.:
693 Influence of C-4 vegetation on (CO_2)-C-13 discrimination and isoforcing in the upper
694 Midwest, United States, Global Biogeochemical Cycles, 24, GB4006
695 doi:10.1029/2009gb003768, 2010.
696 Griffis, T. J., Lee, X., Baker, J. M., Russelle, M. P., Zhang, X., Venterea, R., and Millet, D. B.:
697 Reconciling the differences between top-down and bottom-up estimates of nitrous oxide
698 emissions for the U.S. Corn Belt, Global Biogeochemical Cycles, 27, 746-754,
699 doi:10.1002/gbc.20066, 2013.
700 Haszpra, L., Barcza, Z., Davis, K. J., and Tarczay, K.: Long-term tall tower carbon dioxide flux
701 monitoring over an area of mixed vegetation, Agric. For. Meteorol., 132, 58-77,
702 doi:10.1016/j.agrformet.2005.07.002, 2005.
703 Helliker, B. R., Berry, J. A., Betts, A. K., Bakwin, P. S., Davis, K. J., Denning, A. S., Ehleringer,
704 J. R., Miller, J. B., Butler, M. P., and Ricciuto, D. M.: Estimates of net CO_2 flux by
705 application of equilibrium boundary layer concepts to CO_2 and water vapor measurements

706 from a tall tower, Journal of Geophysical Research-Atmospheres, 109, Artn D20106,
707 doi:10.1029/2004jd004532, 2004.
708 Hernandez-Ramirez, G., Hatfield, J. L., Parkin, T. B., Sauer, T. J., and Prueger, J. H.: Carbon
709 dioxide fluxes in corn-soybean rotation in the midwestern US: Inter- and intra-annual
710 variations, and biophysical controls, Agric. For. Meteorol., 151, 1831-1842,
711 doi:10.1016/j.agrformet.2011.07.017, 2011.
712 Hollinger, S. E., Bernacchi, C. J., and Meyers, T. P.: Carbon budget of mature no-till ecosystem
713 in North Central Region of the United States, Agric. For. Meteorol., 130, 59-69,
714 doi:10.1016/j.agrformet.2005.01.005, 2005.
715 Horst, T. W., and Weil, J. C.: Footprint Estimation for Scalar Flux Measurements in the
716 Atmospheric Surface-Layer, Bound-Lay Meteorol, 59, 279-296, doi:10.1007/Bf00119817,
717 1992.
718 IPCC: 2006 IPCC Guidelines for National Greenhouse Gas Inventories, IGES, Japan, 2006.
719 Jeong, S., Zhao, C., Andrews, A. E., Bianco, L., Wilczak, J. M., and Fischer, M. L.: Seasonal
720 variation of CH_4 emissions from central California, Journal of Geophysical Research-
721 Atmospheres, 117, doi:10.1029/2011jd016896, 2012.
722 Kelliher, F. M., Reisinger, A. R., Martin, R. J., Harvey, M. J., Price, S. J., and Sherlock, R. R.:
723 Measuring nitrous oxide emission rate from grazed pasture using Fourier-transform
724 infrared spectroscopy in the nocturnal boundary layer, Agric. For. Meteorol., 111, 29-38,
725 Pii S0168-1923(02)00007-2, doi:10.1016/S0168-1923(02)00007-2, 2002.
726 Kljun, N., Calanca, P., Rotach, M., and Schmid, H.: A simple parameterisation for flux footprint
727 predictions, Bound-Lay. Meteorol., 112, (3), 503-523, 2004.
728 Knoll, L. B., Vanni, M. J., Renwick, W. H., Dittman, E. K., and Gephart, J. A.: Temperate
729 reservoirs are large carbon sinks and small CO_2 sources: Results from high-resolution
730 carbon budgets, Global Biogeochemical Cycles, 27, 52-64, doi:10.1002/Gbc.20020, 2013.
731 Kort, E. A., Eluszkiewicz, J., Stephens, B. B., Miller, J. B., Gerbig, C., Nehrkorn, T., Daube, B.
732 C., Kaplan, J. O., Houweling, S., and Wofsy, S. C.: Emissions of CH_4 and N_2O over the
733 United States and Canada based on a receptor-oriented modeling framework and COBRA-
734 NA atmospheric observations, Geophys Res Lett, 35, L18808, doi:10.1029/2008gl034031,
735 2008.
736 Kroon, P. S., Hensen, A., Jonker, H. J. J., Ouwersloot, H. G., Vermeulen, A. T., and Bosveld, F.
737 C.: Uncertainties in eddy covariance flux measurements assessed from CH_4 and N_2O
738 observations, Agric. For. Meteorol., 150, 806-816, 2010.
739 Lauvaux, T., Schuh, A. E., Uliasz, M., Richardson, S., Miles, N., Andrews, A. E., Sweeney, C.,
740 Diaz, L. I., Martins, D., Shepson, P. B., and Davis, K. J.: Constraining the CO_2 budget of
741 the corn belt: exploring uncertainties from the assumptions in a mesoscale inverse system,
742 Atmos Chem Phys, 12, 337-354, doi:10.5194/acp-12-337-2012, 2012.
743 Leclerc, M. Y., and Thurtell, G. W.: Footprint Prediction of Scalar Fluxes Using a Markovian
744 Analysis, Bound-Lay Meteorol, 52, 247-258, doi:10.1007/Bf00122089, 1990.

745 Lee, X. H., Massman, W., and Law, B.: Handbook of Micrometeorology: A Guide for Surface
746 Flux Measurement and Analysis, Kluwer Acad., Norwell, Mass, 250 pp., 2004.
747 Levy, P. E., Grelle, A., Lindroth, A., Molder, M., Jarvis, P. G., Kruijt, B., and Moncrieff, J. B.:
748 Regional-scale CO_2 fluxes over central Sweden by a boundary layer budget method, Agric.
749 For. Meteorol., 98-9, 169-180, doi:10.1016/S0168-1923(99)00096-9, 1999.
750 Lin, J. C., Gerbig, C., Wofsy, S. C., Andrews, A. E., Daube, B. C., Davis, K. J., and Grainger, C.
751 A.: A near-field tool for simulating the upstream influence of atmospheric observations:
752 The Stochastic Time-Inverted Lagrangian Transport (STILT) model, Journal of
753 Geophysical Research-Atmospheres, 108, 4493, doi:10.1029/2002jd003161, 2003.
754 Massman, W. J.: A simple method for estimating frequency response corrections for eddy
755 covariance systems, Agric. For. Meteorol., 104, 185-198, doi:10.1016/s0168-
756 1923(00)00164-7, 2000.
757 Mays, K. L., Shepson, P. B., Stirm, B. H., Karion, A., Sweeney, C., and Gurney, K. R.: Aircraft-
758 Based Measurements of the Carbon Footprint of Indianapolis, Environ Sci Technol, 43,
759 7816-7823, doi:10.1021/Es901326b, 2009.
760 Miles, N. L., Richardson, S. J., Davis, K. J., Lauvaux, T., Andrews, A. E., West, T. O., Bandaru,
761 V., and Crosson, E. R.: Large amplitude spatial and temporal gradients in atmospheric
762 boundary layer CO_2 mole fractions detected with a tower-based network in the U.S. upper
763 Midwest, Journal of Geophysical Research-Biogeosciences, 117,
764 doi:10.1029/2011jg001781, 2012.
765 Miller, S. M., Kort, E. A., Hirsch, A. I., Dlugokencky, E. J., Andrews, A. E., Xu, X., Tian, H.,
766 Nehrkorn, T., Eluszkiewicz, J., Michalak, A. M., Wofsy, S. C., Regional sources of
767 nitrous oxide over the United States: Seasonal variation and spatial distribution, Journal of
768 Geophysical Research-Atmospheres, 117, 2012.
769 Morgenstern, K., Black, T. A., Humphreys, E. R., Griffis, T. J., Drewitt, G. B., Cai, T. B., Nesic,
770 Z., Spittlehouse, D. L., and Livingstone, N. J.: Sensitivity and uncertainty of the carbon
771 balance of a Pacific Northwest Douglas-fir forest during an El Nino La Nina cycle, Agric.
772 For. Meteorol., 123, 201-219, doi:10.1016/j.agrformet.2003.12.003, 2004.
773 Moriasi, D. N., Arnold, J. G., Van Liew, M. W., Bingner, R. L., Harmel, R. D., and Veith, T. L.:
774 Model evaluation guidelines for systematic quantification of accuracy in watershed
775 simulations, T Asabe, 50, 885-900, 2007.
776 Nash, J. E., and Sutcliffe, J. V.: River flow forecasting through conceptual models part I — A
777 discussion of principles, Journal of Hydrology, 10, 282-290, doi:10.1016/0022-
778 1694(70)90255-6, 1970.
779 National Research Council: Verifying Greenhouse Gas Emissions: Methods to Support
780 International Climate Agreements, 110 pp., The National Academies Press, Washington,
781 D.C., 2010.

782 Nisbet, E., and Weiss, R.: Top-Down Versus Bottom-Up, Science, 328, 1241-1243,
783 doi:10.1126/science.1189936, 2010.

784 Oda, T. and Maksyutov, S.: A very high-resolution (1 km x 1 km) global fossil fuel
785 CO2 emission inventory derived using a point source database and satellite observations
786 of nighttime lights, Atmos. Chem. Phys., 11, 543-556, doi:10.5194/acp-11-543-2011,
787 2011.
788 Olson, D. M., Griffis, T. J., Noormets, A., Kolka, R., and Chen, J.: Interannual, seasonal, and
789 retrospective analysis of the methane and carbon dioxide budgets of a temperate peatland,
790 Journal of Geophysical Research-Biogeosciences, 118, 226-238, doi:10.1002/Jgrg.20031,
791 2013.
792 Peters, W., Jacobson, A. R., Sweeney, C., Andrews, A. E., Conway, T. J., Masarie, K., Miller, J.
793 B., Bruhwiler, L. M. P., Petron, G., Hirsch, A. I., Worthy, D. E. J., van der Werf, G. R.,
794 Randerson, J. T., Wennberg, P. O., Krol, M. C., and Tans, P. P.: An atmospheric
795 perspective on North American carbon dioxide exchange: CarbonTracker, Proceedings of
796 the National Academy of Sciences of the United States of America, 104, 18925-18930,
797 doi:10.1073/pnas.0708986104, 2007.
798 Ricciuto, D. M., Butler, M. P., Davis, K. J., Cook, B. D., Bakwin, P. S., Andrews, A., and
799 Teclaw, R. M.: Causes of interannual variability in ecosystem-atmosphere CO_2 exchange
800 in a northern Wisconsin forest using a Bayesian model calibration, Agric. For. Meteorol.,
801 148, 309-327, doi:10.1016/j.agrformet.2007.08.007, 2008.
802 Schmid, H. P., Su, H. B., Vogel, C. S., and Curtis, P. S.: Ecosystem-atmosphere exchange of
803 carbon dioxide over a mixed hardwood forest in northern lower Michigan, Journal of
804 Geophysical Research-Atmospheres, 108, doi:10.1029/2002jd003011, 2003.
805 Striegl, R. G., and Michmerhuizen, C. M.: Hydrologic influence on methane and carbon dioxide
806 dynamics at two north-central Minnesota lakes, Limnol Oceanogr, 43, 1519-1529, 1998.
807 Suyker, A. E., Verma, S. B., and Burba, G. G.: Interannual variability in net CO_2 exchange of a
808 native tallgrass prairie, Global Change Biol, 9, 255-265, doi:10.1046/J.1365-
809 2486.2003.00567.X, 2003.
810 Tang, X. G., Wang, Z. M., Liu, D. W., Song, K. S., Jia, M. M., Dong, Z. Y., Munger, J. W.,
811 Hollinger, D. Y., Bolstad, P. V., Goldstein, A. H., Desai, A. R., Dragoni, D., and Liu, X.
812 P.: Estimating the net ecosystem exchange for the major forests in the northern United
813 States by integrating MODIS and AmeriFlux data, Agric. For. Meteorol., 156, 75-84,
814 doi:10.1016/j.agrformet.2012.01.003, 2012.
815 U.S. EPA: Inventory of U.S. Greenhouse Gas Emissions and Sinks: 1990–2012, 529 pp.,
816 Washington, D.C., 2014.
817 Ussiri, D. A. N., Lal, R., and Jarecki, M. K.: Nitrous oxide and methane emissions from long-
818 term tillage under a continuous corn cropping system in Ohio, Soil Till Res, 104, 247-255,
819 doi:10.1016/J.Still.2009.03.001, 2009.
820 Vesala, T., Kljun, N., Rannik, Ü., Rinne, J., Sogachev, A., Markkanen, T., Sabelfeld, K., Foken,
821 T., and Leclerc, M.: Flux and concentration footprint modelling: State of the art, Environ.
822 Pollut., 152, (3), 653-666, 2008.

Werner, C., Davis, K., Bakwin, P., Yi, C. X., Hurst, D., and Lock, L.: Regional-scale measurements of CH_4 exchange from a tall tower over a mixed temperate/boreal lowland and wetland forest, Global Change Biol, 9, 1251-1261, 2003.

West, T. O., Bandaru, V., Brandt, C. C., Schuh, A. E., and Ogle, S. M.: Regional uptake and release of crop carbon in the United States, Biogeosciences, 8, 2037-2046, doi:10.5194/bg-8-2037-2011, 2011.

Williams, I. N., Riley, W. J., Torn, M. S., Berry, J. A., and Biraud, S. C.: Using boundary layer equilibrium to reduce uncertainties in transport models and CO_2 flux inversions, Atmos Chem Phys, 11, 9631-9641, doi:10.5194/acp-11-9631-2011, 2011.

Wunch, D., Wennberg, P. O., Toon, G. C., Keppel-Aleks, G., and Yavin, Y. G.: Emissions of greenhouse gases from a North American megacity, Geophys Res Lett, 36, Artn L15810, doi:10.1029/2009gl039825, 2009.

Xiao, J. F., Zhuang, Q. L., Baldocchi, D. D., Law, B. E., Richardson, A. D., Chen, J. Q., Oren, R., Starr, G., Noormets, A., Ma, S. Y., Verma, S. B., Wharton, S., Wofsy, S. C., Bolstad, P. V., Burns, S. P., Cook, D. R., Curtis, P. S., Drake, B. G., Falk, M., Fischer, M. L., Foster, D. R., Gu, L. H., Hadley, J. L., Hollinger, D. Y., Katul, G. G., Litvak, M., Martin, T. A., Matamala, R., McNulty, S., Meyers, T. P., Monson, R. K., Munger, J. W., Oechel, W. C., U, K. T. P., Schmid, H. P., Scott, R. L., Sun, G., Suyker, A. E., and Torn, M. S.: Estimation of net ecosystem carbon exchange for the conterminous United States by combining MODIS and AmeriFlux data, Agric. For. Meteorol., 148, 1827-1847, doi:10.1016/j.agrformet.2008.06.015, 2008.

Yi, C., Davis, K. J., Bakwin, P. S., Berger, B. W., and Marr, L. C.: Influence of advection on measurements of the net ecosystem-atmosphere exchange of CO_2 from a very tall tower, Journal of Geophysical Research-Atmospheres, 105, 9991-9999, doi:10.1029/2000jd900080, 2000.

Yi, C., Davis, K. J., Bakwin, P. S., Denning, A.S., Zhang, N., Desai, A., Lin, J. C., and Gerbig, C.: The observed covariance between ecosystem carbon exchange and atmospheric boundary layer dynamics at a site in northern Wisconsin, Journal of Geophysical Research, 109, D08302, doi:10.1029/2003JD004164, 2004.

Yi, C. X., Davis, K. J., Berger, B. W., and Bakwin, P. S.: Long-term observations of the dynamics of the continental planetary boundary layer, J Atmos Sci, 58, 1288-1299, doi:10.1175/1520-0469(2001)058<1288:Ltootd>2.0.Co;2, 2001.

Zhang, X.: Improving regional-scale greenhouse gas inventories in an agriculture-dominated landscape using a multi-scale approach, PhD Dissertation, Yale University, 2013.

Zhang, X., Lee, X., Griffis, T., Baker, J., Erickson, M., Hu, N., and Xiao, W.: The influence of plants on atmospheric methane in an agriculture-dominated landscape, Int J Biometeorol, 1-15, doi:10.1007/s00484-013-0662-y, 2013.

Zhang, X., Lee, X., Griffis, T., Andrews, A., Baker, J., Erickson, M., Hu, N., and Xiao, W.: Quantifying nitrous oxide fluxes on multiple spatial scales in the Upper Midwest, USA, Int J Biometeorol, 1-15, doi: 10.1007/s00484-014-0842-4, 2014.

Zhao, C. F., Andrews, A. E., Bianco, L., Eluszkiewicz, J., Hirsch, A., MacDonald, C., Nehrkorn, T., and Fischer, M. L.: Atmospheric inverse estimates of methane emissions from Central California, Journal of Geophysical Research-Atmospheres, 114, doi:10.1029/2008jd011671, 2009.

Zhuang, Q. L., Lu, Y. Y., and Chen, M.: An inventory of global N_2O emissions from the soils of natural terrestrial ecosystems, Atmos Environ, 47, 66-75, doi:10.1016/j.atmosenv.2011.11.036, 2012.

Tables

Table 1. Correlation coefficient and NSE (Nash-Sutcliffe efficiency) between EC flux and the other two methods. CT denotes CarbonTracker, and FA denotes the flux aggregation method.

Distance		5 km	10 km	20 km	50 km	100 km	200 km	300 km	600 km
CT	**NSE**	NA	NA	NA	NA	0.41	0.82	0.92	0.97
	r	NA	NA	NA	NA	0.96	0.97	0.98	0.99
FA	**NSE**	0.48	0.49	0.37	0.23	0.58	0.90	0.95	0.96
	r	0.98	0.98	0.98	0.98	0.98	0.98	0.98	0.98

874 Table 2. A summary of annual NEE estimated from different methods. NEE in the "Reference" column is from the study in Midwest
875 US in recent years. Negative fluxes indicate carbon sink from the atmosphere and positive fluxes indicate carbon release to the
876 atmosphere.

	This study ($g C-CO_2 m^{-2} yr^{-1}$)	Reference ($g C-CO_2 m^{-2} yr^{-1}$)
Tall tower Eddy Covariance	-131 ± 35	120 ± 140 (1997-2004) (Ricciuto et al., 2010) 16 ± 19 (1997) (Davis et al., 2003) -71 (2000) (Helliker et al., 2004) 16 (1997) (Bakwin et al., 2004)
CarbonTracker	-54 ± 12	-58 (2000-2006) (Desai et al., 2010)
Equilibrium	46-74	-110 ± 14 (1997-2006) (Desai et al., 2010) -38 (2000) (Helliker et al., 2004) 79 (1997) (Bakwin et al., 2004)
Flux Aggregation	-130 ± 34	
Corn	-599 ± 26	-466 ± 38 (2004-2007) (Hernandez-Ramirez et al., 2011) -576 ± 101 (1997-2002) (Hollinger et al., 2005)
Soybean	10 ± 18	-13 ± 39 (2004-2007) (Hernandez-Ramirez et al., 2011) -32 ± 161 (1997-2002) (Hollinger et al., 2005)
Grassland	-411 ± 10	-148 ± 116 (1997-1999) (Suyker et al., 2003)
Forest	-227 ± 14	-137 ± 49 (1999-2001) (Schmid et al., 2003)
Fossil fuel	124± 12	
Other methods		
Interannual Flux Tower Upscaling Experiment		-321 ± 13 (1997-2006) (Desai et al., 2010)
Mesoscale inverse modeling		-183 ± 35 (1997-2006) (Lauvaux et al., 2012)

877 **Figures**

878

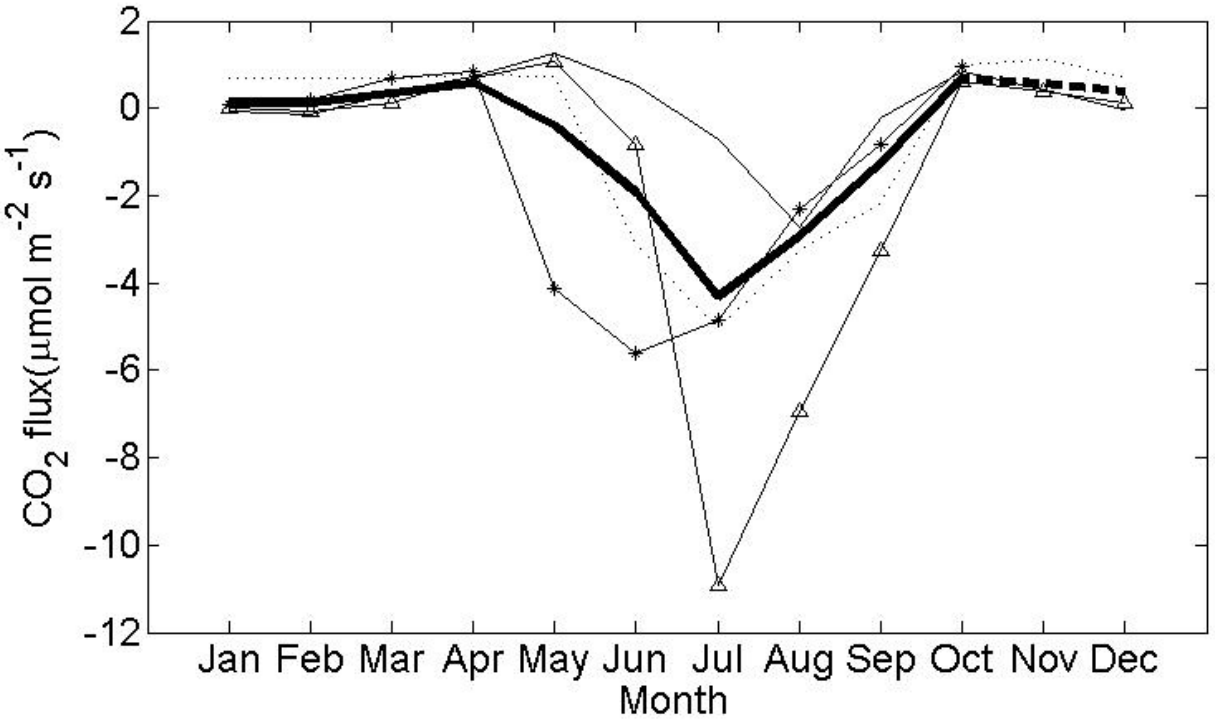

879

880 Figure 1. The biogenic CO_2 flux (thick solid line) from the landscape around the tall tower, calculated from monthly averages of CO_2
881 flux from major land cover types. The fluxes for corn (solid line with triangles) and soybean (thin solid line) were measured with eddy
882 covariance tower at the G21 and G19 site near the tall tower in Minnesota. The fluxes for forest (dotted line) and grassland (solid line
883 with stars) were from UMBS and USIB2 AmeriFlux sites in North America.

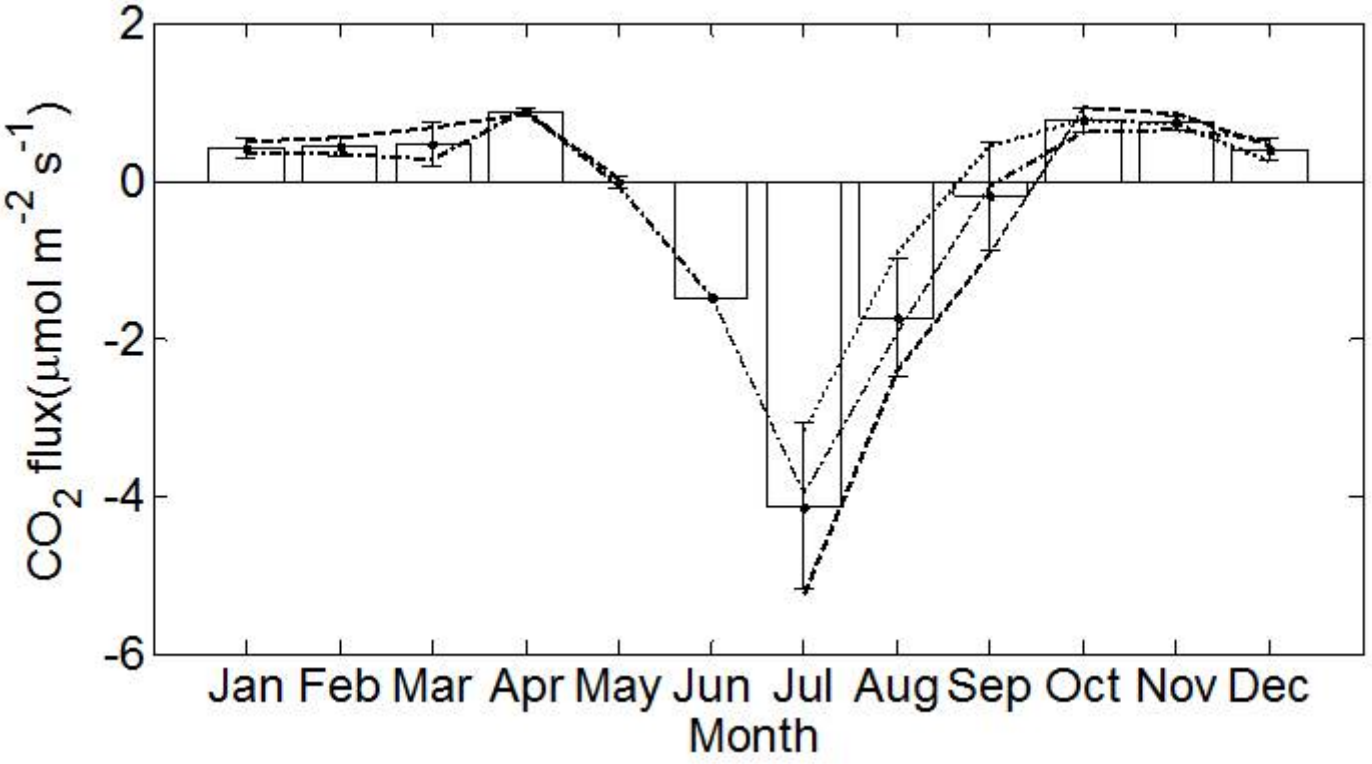

884

885 Figure 2. Monthly averages of CO_2 flux in 2007 (dotted line), 2008 (dot-dashed line), and 2009 (dashed line) measured with EC on the
886 tall tower. White bars are the mean monthly value from the available data during the three-year observation period. Error bars on the
887 top of white bars show the lower and upper boundary of the three-year measurements for each month.

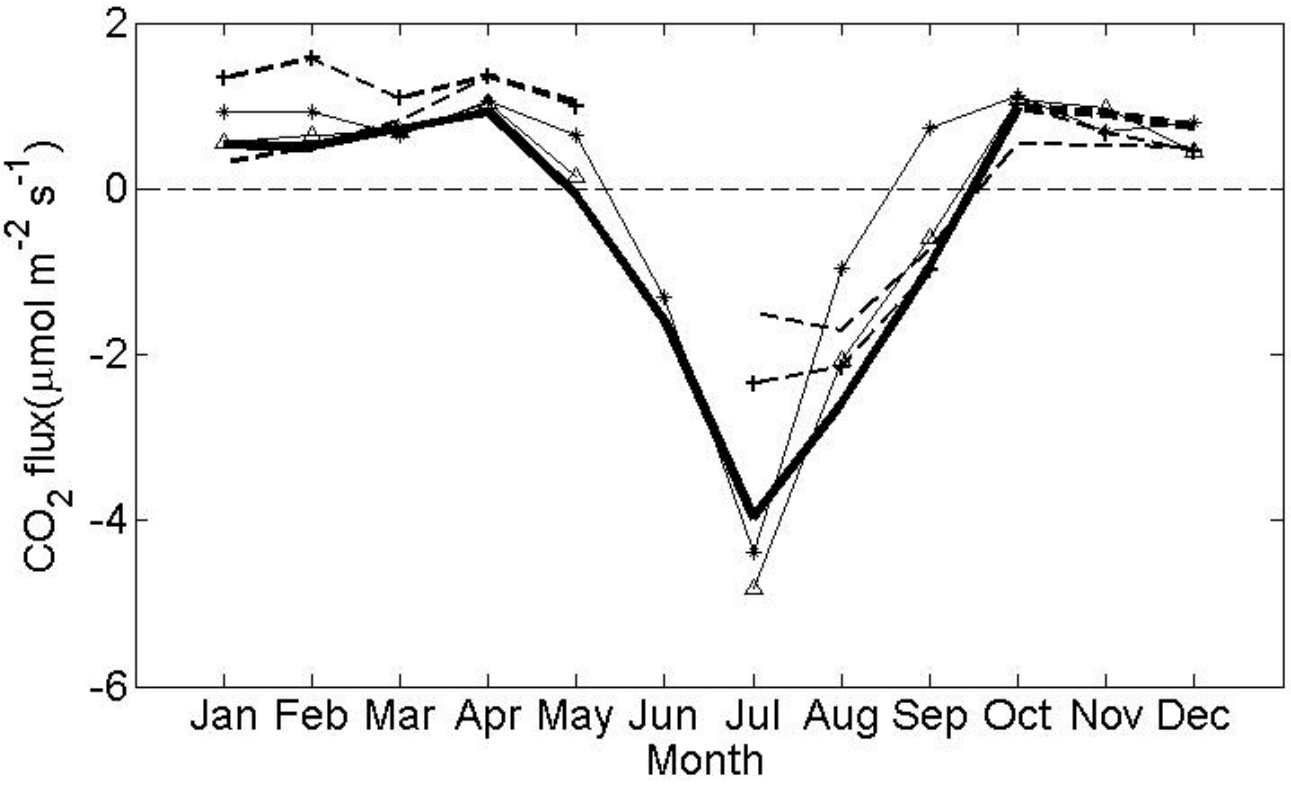

888

889 Figure 3. Monthly CO_2 flux in 2009 estimated with flux aggregation (FA, thick solid line), eddy covariance method (F_{EC}, line with
890 triangles), CarbonTracker (F_{CT}, line with stars), equilibrium method with H_2O as a tracer (F_{EH}, thin dashed line), and equilibrium
891 method using NCEP reanalysis data (F_{EO}, thin dashed line with cross). The FA flux ended in October because the grassland data was
892 missing in November and December. The missing FA flux was determined by assuming the missing grassland flux in November and
893 December was the same as October flux (thick dashed line).

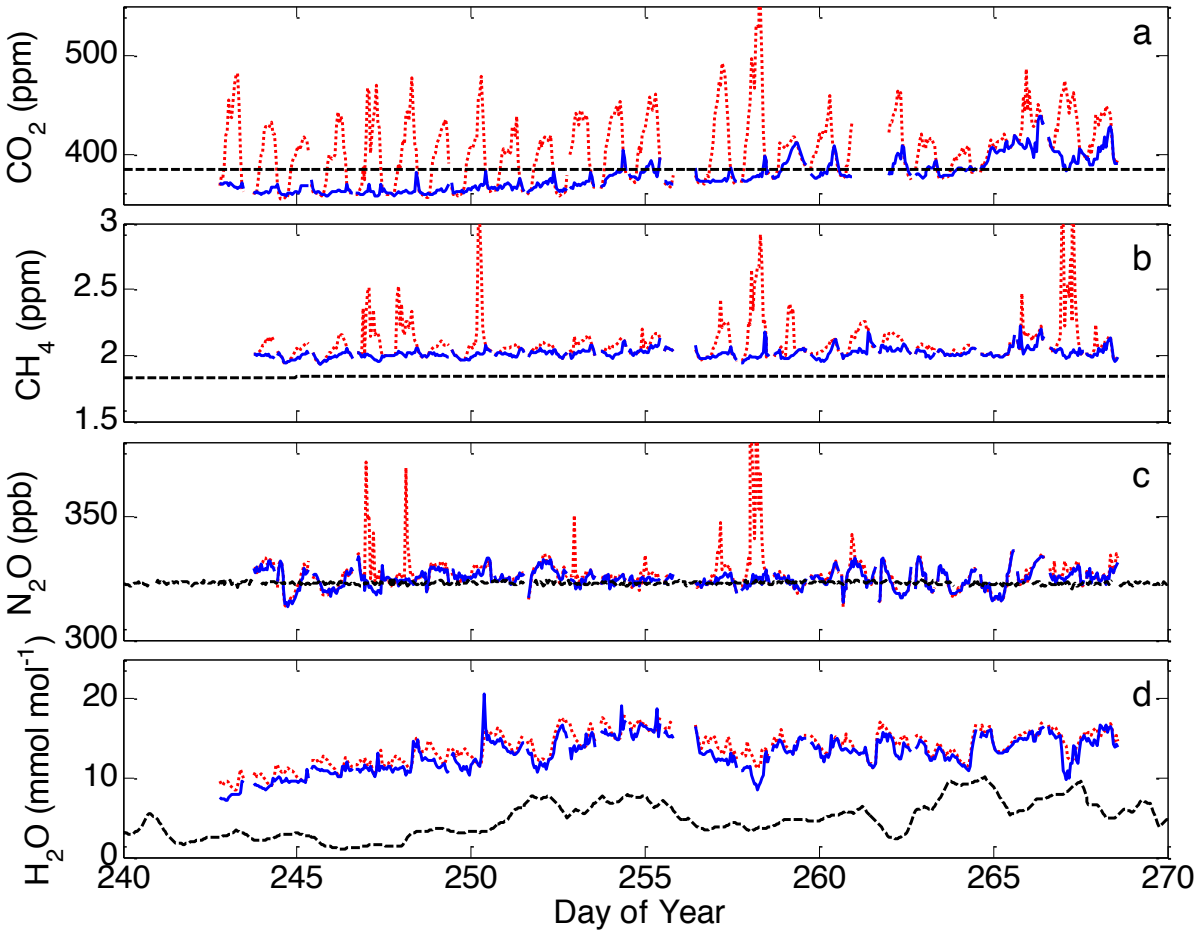

894

895 Figure 4. Hourly averages of CO_2 (a), CH_4 (b), N_2O (c), and H_2O (d) mixing ratio during the observation period from DOY 243 to

896 DOY 269, 2009. Blue solid line— mixing ratio on 200 m. Red dotted line— mixing ratio on 3 m. Black dashed line— mixing ratio at

897 Niwot Ridge site.

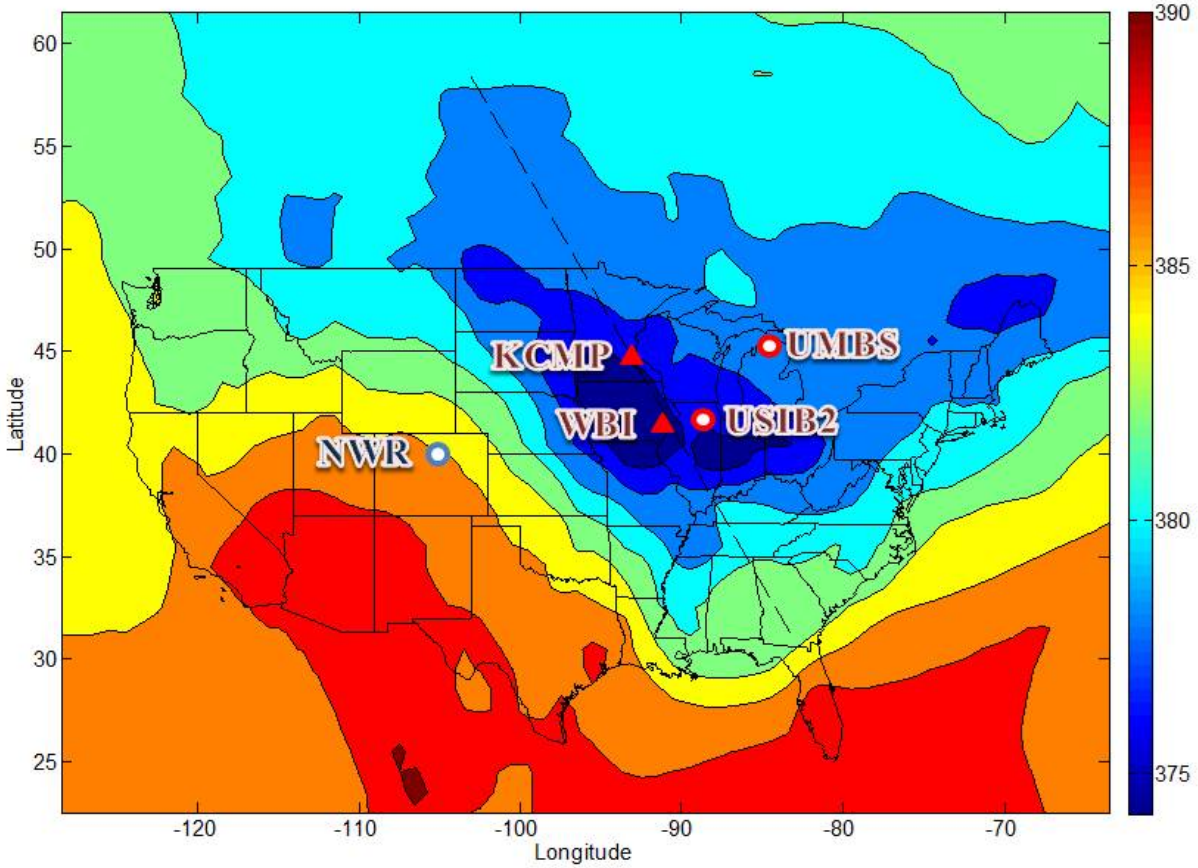

898

899 Figure 5. CO_2 concentration averaged from land surface to 1274.1 m according to the CarbonTracker 3D CO_2 concentration product in
900 July, 2009. Dashed line — previling wind direction in July from northwest to southeast. Red triangle — the KCMP tower site and
901 WBI tower obserservotory operated by NOAA. Red circle— Ameriflux sites. Blue circle — background observation site. The color
902 scale is the CO_2 concentration in ppm. The resolution of the concentration data is 1° by 1°.